

Compton Double Ionization of Helium in the Region of the Cross-Section Maximum

B. Krässig,^{1,*} R. W. Dunford,¹ D. S. Gemmell,¹ S. Hasegawa,^{1,†} E. P. Kanter,¹ H. Schmidt-Böcking,²
W. Schmitt,^{3,1} S. H. Southworth,¹ Th. Weber,^{2,1} and L. Young¹

¹Argonne National Laboratory, Argonne, Illinois 60439

²Institut für Kernphysik, Universität Frankfurt, August-Euler-Straße 6, D-60486 Frankfurt, Germany

³Fakultät für Physik, Universität Freiburg, D-79104 Freiburg, Germany

(Received 22 March 1999)

The ratio of double-to-single ionization in helium by Compton scattering has been measured in the 8–28 keV x-ray energy range. The ratio attains a maximum value of 1.6% near 13 keV before descending towards the high-energy asymptotic region. The reported results resolve the discrepancies among previously published theoretical and experimental work in this energy range. The present data are most closely approximated by the results of the many-body perturbation theory calculation of Bergstrom *et al.* [Phys. Rev. A **51**, 3044 (1995)].

PACS numbers: 32.80.Cy

There exist substantial discrepancies between theoretical predictions for the cross section of double ionization in helium by Compton scattering. Consistency between different approaches has been reached for the high-energy asymptotic value of the double-to-single ionization ratio $R_C = \sigma_C^{2+}/\sigma_C^+$ (cf. [1], and references therein), but the available theoretical results differ strongly in their predictions for the energy dependence of R_C leading up to this limit. The sparsity and large uncertainty of published experimental results have previously prohibited a conclusive assessment of any of these predictions. The main impediment to experimental determinations of R_C arises from the smallness of the Compton cross section of about 10^{-24} cm². The fundamental difficulty for theoretical treatments lies in accounting adequately for electron correlation in the initial bound and final continuum states of the system. Part of this difficulty is circumvented in the impulse approximation (IA), where only a correlated initial-state wave function is needed in the calculation. At energies as low as 6 keV the x-ray inelastic scattering cross section for helium calculated in this way agrees within a few percent with the experiment [2]. For the double-ionization channel, however, the calculation in IA [3] is least favored by the experimental data and recent work estimates it to become adequate only above 50 keV [4]. In the effort to include final-state correlation, substantial progress has been made for the corresponding case in photoabsorption (cf. [5], and references therein), where, in contrast to Compton scattering, the transfer of energy and angular momentum are well defined and fixed. Since the recent review of McGuire *et al.* [6], advances have also been made in relating the findings for helium double ionization by photons and charged particle collisions [7]. We report here precise experimental results for the ratio R_C in the 8–28 keV x-ray energy range which allow a critical evaluation of theoretical predictions.

The experiment was performed at the Basic Energy Sciences Synchrotron Radiation Center (BESSRC) undulator

beam line 12-ID at the Advanced Photon Source (APS). The collimated x-ray beam (5×3 mm²) entered and exited the vacuum chamber through 127- μ m-thick beryllium windows. Inside the vacuum chamber the x-ray beam intersected a jet of cold helium atoms created by skimmed supersonic expansion. In the interaction region the jet measured 5 mm in diameter and possessed an areal density of about 5×10^{12} cm⁻². The residual gas pressure in the chamber was 10^{-7} Torr. The vacuum chamber further held a time-of-flight (TOF) spectrometer in a 160° reflectron geometry with 40 cm flight path. The dc extraction field across the interaction region was 177 V/cm, and the total acceleration potential along the flight path to the detector was 2.9 kV. The electrostatic reflector in the flight path of the ions effectively eliminated prompt counts on the detector caused by scattered x rays and energetic electrons from the interaction region. The detector consisted of a set of three multichannel plates (MCP) in a “Z-stack” arrangement with a two-dimensionally position-sensitive “wedge-and-strip” anode. Time-of-flight measurements were made relative to the time structure of the storage-ring fill pattern. The combination of a cold and spatially confined target, a TOF spectrometer with a position-sensitive detector, and event-mode data acquisition constitutes a COLTRIMS system (cold target recoil ion momentum spectroscopy [8]). Here, this technique was employed to distinguish Compton ionization events from photoabsorption events by means of their different recoil momenta. Whereas in photoabsorption the ion recoils from the emission of photoelectrons, virtually no momentum is transferred to the residual ion in Compton scattering (cf. [9]).

Taking a vanishing ion recoil momentum as a sign that the x ray had been scattered rather than absorbed is strictly valid for the case of single ionization; in double photoionization this concept is applicable only under the condition that the two outgoing photoelectrons give the ion an appreciable net recoil momentum, for instance, when the

energy sharing between them is strongly asymmetric. In the current understanding of double ionization by photoabsorption of keV x rays, the two emitted electrons actually do emerge most probably with very different kinetic energies (see, e.g., Ref. [10]). However, the same is not true for the absorption mechanism proposed by Drukarev [11] in which the momentum transfer to the doubly charged ion would be very small. To date this effect has not been observed. In the present experiment, these events would be counted wrongly as originating from Compton scattering. However, in the magnitude estimated in [11], such photoabsorption events would amount to less than 1% of the Compton double-ionization events and their effect on the measured ratio R_C would be much smaller than the experimental uncertainty.

Measurements were carried out at 8, 10, 13, 16, 20, 24, and 28 keV, using the Si(111) reflection in a double-crystal monochromator. By deliberately detuning the second crystal in the monochromator slightly off the maximum in the transmission curve, the intensity of higher-order contributions in the monochromatized x-ray beam could be effectively suppressed. The five lower energies were measured during timing mode operation of the storage ring (20 single pulses in 130 ns intervals, 3.7 μ s repetition time), and the 24 and 28 keV measurements were performed using the regular APS fill pattern (25 triplet pulses with 2.8 ns spacings in 102 ns intervals, same repetition time). The microsecond-time scale ion flight times in conjunction with the short intervals between subsequent x-ray pulses caused the TOF spectrum to multiply overlap itself. Special care was taken in choosing the spectrometer operating parameters to ensure that the He TOF peaks (<2 ns FWHM) were not superimposed on other structures in the spectrum. The portions in the total TOF spectrum resulting from the 20 single pulses

(25 triplet pulses) were added up in the analysis into single TOF spectra for the two He charge states (see Fig. 1). Typical accumulation times were 6–8 h per energy with target gas and a comparable period without gas to determine the background TOF spectrum at each energy. The background originated from dark counts and ionization of residual gas constituents. The background spectra were mildly structured, and they became weaker and flatter with increasing x-ray energy; in particular, there was no indication of H_2^+ ions which might underlie the He^{2+} events due to their equal q/m ratios.

For the purpose of selecting out the Compton events in the recorded data, only those counts on the position-sensitive detector were accumulated into TOF spectra as in Fig. 1 which lay inside a small octagonal window around the region where the centroid trajectory met the detector plane, i.e., ions with small momentum components perpendicular to the flight path. In the resulting TOF spectra only those counts in narrow windows around the maximum in the He TOF peaks were counted (see Fig. 1), i.e., ions with small momentum components in the direction of the flight path and, consequently, with small total recoil momenta. In the determination of the He charge-state ratio several different window sizes were tried and no systematic trends or variations outside statistical uncertainties were detected.

An important aspect in the determination of the charge-state ratio is the dependence of the MCP detection efficiency on the ion impact energy (see, e.g., Ref. [12]). After electrostatic extraction and acceleration, the doubly charged He^{2+} ions impinge on the MCP surface with twice the energy of the He^+ ions, thereby enhancing the yield of secondary emission. Using a pulsed electron gun as an ionization source and with careful run-to-run normalization, we found an increase of a few percent in the count rates of the helium charge states when raising the acceleration potential from 2.9 to 5.8 kV. The effect of equalizing the impact energies is reflected in the resulting pulse-height distributions shown in Fig. 2. The pulse-height distribution of He^{2+} ions accelerated by 2.9 kV potential (open circles) differs from that of He^+ ions accelerated in the same potential (open triangles), but it is perfectly replicated by the He^+ distribution with 5.8 kV accelerating potential (solid triangles). Repeating this measurement at different stages of the experiment over a period of a few months, we noticed as a result of aging of the MCPs not only a decrease in the gain, but also a gradual deterioration in the relative detection efficiencies. The efficiency ratio $\rho^+ = He^+$ at 2.9 kV/ He^+ at 5.8 kV decreased from 0.974(3) to 0.927(3) during this period. Averaged over several determinations, the corresponding detection-efficiency ratio ρ^{2+} for He^{2+} was found to be 0.985(15), showing that a plateau in the detection-efficiency dependence had almost been reached at 5.8 keV impact energy. The ion-count ratios He^{2+}/He^+ recorded with 2.9 kV acceleration potential were corrected with the efficiency factors ρ^+

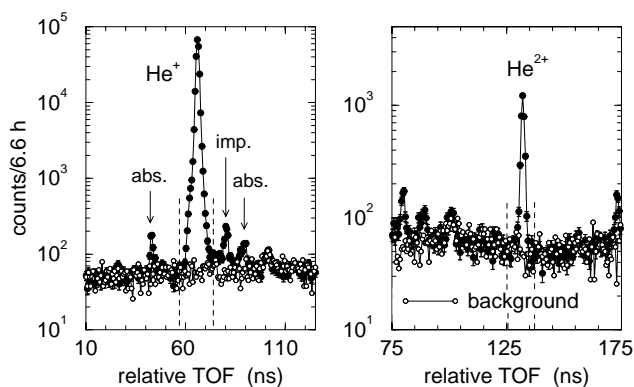


FIG. 1. Compounded TOF spectra for He^+ and He^{2+} ions with small momenta perpendicular to the flight path, measured with 16 keV x rays, points with error bars; background measurement, open circles; integration limits for Compton events, dashed lines. The arrows indicate the remnants of forward/backward recoiling He^+ from photoabsorption (abs.) and He^+ counts created by a bunch impurity in the storage-ring fill pattern (imp.).

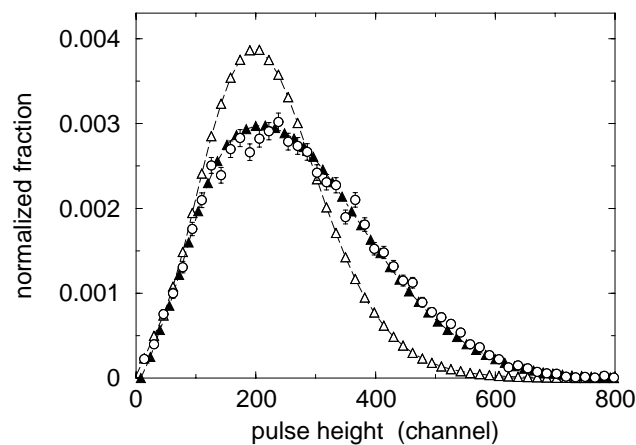


FIG. 2. Normalized pulse-height distributions of the Z-stack MCP detector for different ion impact energies. He^+ at 2.9 keV, open triangles; He^+ at 5.8 keV, solid triangles; He^{2+} at 5.8 keV, open circles.

measured nearest in time to reflect the true cross-section ratios.

Figure 3 shows a comparison of our measured values for the ratio $R_C = \sigma_C^{2+} / \sigma_C^+$ in helium (open circles) with published experimental and theoretical results. The present data are highlighted by the shaded band, which is a smooth curve fitted to the data points and broadened by the experimental uncertainty. The shaded band represents our result for the energy dependence $R_C(E)$ in helium. It traverses the considerable scatter of prior experimental data in this region [9,15–18] and suggests a smooth connection with the recent high-energy data of Spielberger *et al.* (solid circles [13,14]) which indicate a very flat behavior of $R_C(E)$ above 40 keV x-ray energy. At the lower end of our range the data agree with the earlier measurement of Spielberger *et al.* [9] and with recently reported results by Becker *et al.* (triangles down [18]). In the latter experiment no distinction between photoabsorption and Compton ionization events was made. We include in Fig. 3 their data points above 9 keV. The authors of Ref. [18] estimated the deviation in these points caused by photoabsorption events to be smaller than the respective error bars.

Among the theoretical predictions of $R_C(E)$ the present experiment favors most the result of the many-body perturbation theory (MBPT) calculation by Bergstrom *et al.* (solid curve [20]), which lies 5%–10% higher than the shaded band. At 20 keV the discrepancy is greater and the experimental result decreases more rapidly with energy than the apparent trend in the MBPT results. From about 10 keV upwards our R_C values lie substantially higher than the results of Andersson and Burgdörfer [21], who performed their calculation with two different choices of correlated final-state wave functions (short-dashed and dot-dashed curves). This underestimation persists, to a lesser degree, in the improved extension of that work above 20 keV (long-dashed curve [14]). In the energy range cov-

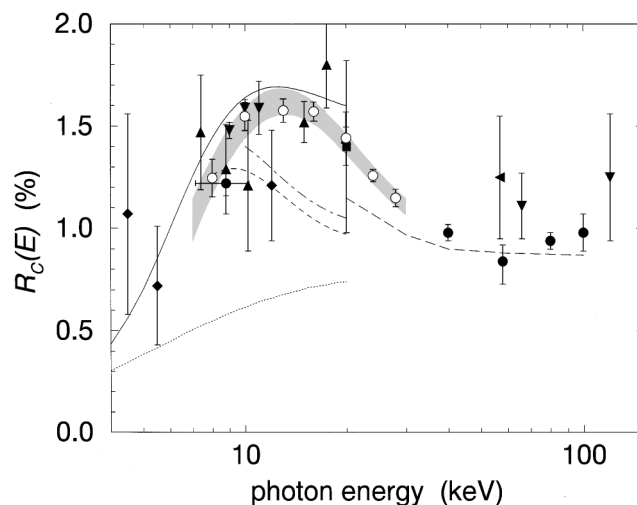


FIG. 3. Experimental and theoretical results for $R_C(E)$. This work, open circles; the shaded band is a smooth curve fitted to the data and broadened by the experimental uncertainty. Other experiments: Spielberger *et al.* [9,13,14], solid circles; Levin *et al.* [15], triangles up; Morgan and Bartlett [16], diamonds; Samson *et al.* [17], square; Becker *et al.* [18], triangles down; Wehlitz *et al.* [19], triangle left. Theory: Bergstrom *et al.* [20], MBPT, solid curve; Andersson and Burgdörfer [21], 3C final state, short-dashed curve, and Byron-Joachain type CI final state, dot-dashed curve; Spielberger *et al.* [14], 3C final state, long-dashed curve; Surić *et al.* [3], IA, dotted curve.

ered by the present experiment this discrepancy may be attributed to the substantial fractions of Compton scattering events in which the energy transfers are below 1 keV. The 3C approach (a product of three Coulomb functions in the final state) used in the two latter references is believed to be less accurate for such lower energy transfers [14,22]. In the calculation based on the IA the maximum in $R_C(E)$ is absent (dotted curve [3]). This calculation clearly fails to describe $R_C(E)$ in the energy range of the present experiment. As mentioned above, it was recently estimated that use of the IA for the calculation of the helium double-ionization cross section should be adequate only above about 50 keV [4].

Using tabulated results for the total incoherent scattering cross section [23], our experimental data have been converted into cross sections σ_C^{2+} for double ionization by Compton scattering (Fig. 4). Following the onset, the energy dependence of σ_C^{2+} exhibits a clear maximum at about 14 keV x-ray energy before falling off at higher energies. The figure also contains the result of the MBPT calculation (solid line [20]) which best approximates the features and magnitude of the measured double-ionization cross section. The energy dependence of σ_C^{2+} is somewhat reminiscent of the curve shown in Ref. [20] which was obtained by using in the calculation just the particular single term commonly referred to as “TS1” (dashed line). This term is one of the four first-order terms and, together with a second term, it is associated with correlation in the final state. In the generalized length formulation used in

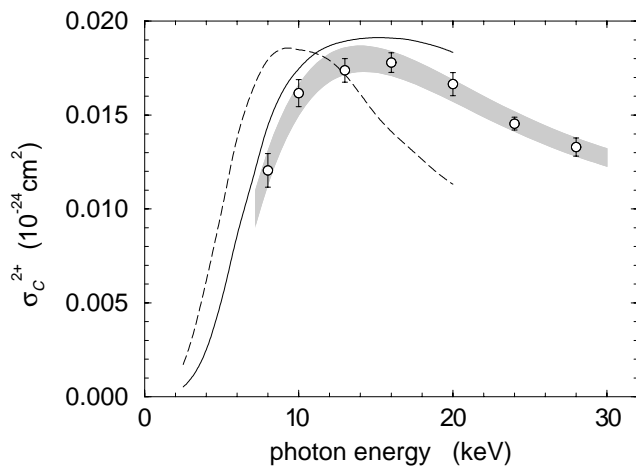


FIG. 4. Compton double-ionization cross section in helium. This work, open circles and shaded band; Bergstrom *et al.* [20], full MBPT calculation, solid curve; contribution of TS1 amplitude, dashed curve.

Ref. [20], this term gives the biggest contribution to σ_C^{2+} , and it is the only term exhibiting a maximum in the energy dependence. Nonetheless, all four terms must be taken into account in the calculation, and the coherent addition of all four terms as well as a different choice of gauge are bound to modify the individual contributions. We expect the reported experimental results to be a helpful guide in the necessary refinement of theoretical treatments of this fundamentally important process.

In summary, we report precise experimental data on the ratio of double-to-single ionization in helium by Compton scattering in the range of 8–28 keV x-ray energy. In contrast to previously published data sets, our results clearly delineate the energy dependence of this quantity in the investigated range and show the existence of a maximum in the Compton double-ionization cross section near 14 keV. Among the published theoretical predictions for this energy range our results favor most the calculation based on the MBPT, which reproduces the shape of the cross-section maximum, but overestimates our data by about 5%–10%. The deviation between experiment and calculation increases with energy. No theoretical calculation is currently able to reproduce the observed energy dependence of the ratio between the maximum and recently published high-energy data points.

We thank U. Becker and J. Levin for communicating their results prior to publication. We are grateful to the BESSRC staff for excellent research facilities and their assistance during the experiment. H.S.B. and T.W. acknowledge support by the Deutsche Forschungsgemeinschaft and the German Bundesministerium für Bildung

und Forschung. This work was supported by the U.S. Department of Energy, Office of Science, Division of Chemical Sciences and Division of Nuclear Physics (D. S. G.) under Contract No. W-31-109-Eng-38.

*Corresponding author.

Email address: kraessig@anl.gov

†Present address: Department of Quantum Engineering and System Science, University of Tokyo, Tokyo, Japan

- [1] T. Surić, K. Pisk, and R.H. Pratt, *Phys. Lett. A* **211**, 289 (1996).
- [2] G.E. Ice, M.H. Chen, and B. Crasemann, *Phys. Rev. A* **17**, 650 (1978).
- [3] T. Surić, K. Pisk, B. A. Logan, and R.H. Pratt, *Phys. Rev. Lett.* **73**, 790 (1994).
- [4] Z. Kaliman, T. Surić, K. Pisk, and R.H. Pratt, *Phys. Rev. A* **57**, 2683 (1998).
- [5] J. A. R. Samson *et al.*, *Phys. Rev. A* **57**, 1906 (1998).
- [6] J.H. McGuire *et al.*, *J. Phys. B* **28**, 913 (1995).
- [7] J.H. McGuire, J. Wang, and J. Burgdörfer, *Phys. Rev. A* **54**, 3668 (1996); J. Wang, J.H. McGuire, J. Burgdörfer, and Y. Qiu, *ibid.* **54**, 613 (1996); *Phys. Rev. Lett.* **77**, 1723 (1996).
- [8] J. Ullrich *et al.*, *J. Phys. B* **30**, 2917 (1997).
- [9] L. Spielberger *et al.*, *Phys. Rev. Lett.* **74**, 4615 (1995).
- [10] Ken-ichi Hino *et al.*, *Phys. Rev. A* **48**, 1271 (1993).
- [11] E.G. Drukarev, *Phys. Rev. A* **51**, R2684 (1995).
- [12] B. Brehm, J. Grosser, T. Ruschinski, and M. Zimmer, *Meas. Sci. Technol.* **6**, 953 (1995).
- [13] L. Spielberger *et al.*, *Phys. Rev. Lett.* **76**, 4685 (1996).
- [14] L. Spielberger *et al.*, *Phys. Rev. A* **59**, 371 (1999).
- [15] J.C. Levin, G.B. Armen, and I.A. Sellin, *Phys. Rev. Lett.* **76**, 1220 (1996).
- [16] D.V. Morgan and R.J. Bartlett, *Phys. Rev. A* **59**, 4075 (1999).
- [17] J.A.R. Samson, Z.X. He, W. Stolte, and J.N. Cutler, *J. Electron Spectrosc. Relat. Phenom.* **78**, 19 (1996).
- [18] U. Becker *et al.*, *Aust. J. Phys.* (to be published). Results shown are weighted means of data points within $E \pm 0.3$ keV.
- [19] R. Wehlitz *et al.*, *Phys. Rev. A* **53**, 3720 (1996).
- [20] P.M. Bergstrom, Jr., K. Hino, and J. Macek, *Phys. Rev. A* **51**, 3044 (1995).
- [21] L.R. Andersson and J. Burgdörfer, *Phys. Rev. A* **50**, R2810 (1994).
- [22] Y. Qiu, J.-Z. Tang, and J. Burgdörfer, *Phys. Rev. A* **57**, R1480 (1998).
- [23] M.J. Berger and J.H. Hubbell, NIST Standard Reference Database 8 (XGAM), NBSIR 87-3597, available under <http://physics.nist.gov/PhysRefData/Xcom/Text/XCOM.html>. Raman scattering has been neglected in the conversion of total incoherent scattering to double ionization.